

<sup>1</sup> Traits predict forest phenological responses to photoperiod  
<sup>2</sup> more than temperature

<sup>3</sup> Deirdre Loughnan<sup>1</sup>, Faith A M Jones<sup>1, 2</sup>, and E M Wolkovich<sup>1,3,4</sup>

<sup>4</sup> January 4, 2026

<sup>5</sup> <sup>1</sup> Department of Forest and Conservation, Faculty of Forestry, University of British Columbia, 2424  
<sup>6</sup> Main Mall Vancouver, BC Canada V6T 1Z4.

<sup>7</sup> <sup>2</sup> Department of Wildlife, Fish and Environmental Studies, Swedish University of Agricultural Sci-  
<sup>8</sup> ences, 901 83 Umeå, Sweden.

<sup>9</sup> <sup>3</sup> Arnold Arboretum of Harvard University, 1300 Centre Street, Boston, Massachusetts, USA;

<sup>10</sup> <sup>4</sup> Organismic & Evolutionary Biology, Harvard University, 26 Oxford Street, Cambridge, Massachusetts,  
<sup>11</sup> USA;

<sup>12</sup> Corresponding Author: Deirdre Loughnan deirdre.loughnan@ubc.ca

<sup>13</sup> Running title: Traits drive photoperiod cues in budburst

<sup>14</sup> **Summary**

<sup>15</sup> As the timing of plant life cycle events—phenology—has shifted with climate change, there is growing  
<sup>16</sup> interest to incorporate phenology within plant strategies has received growing interest as phenology  
<sup>17</sup> has shifted with climate change. But integrating phenology into to existing spectra (like the leaf  
<sup>18</sup> economic spectrum and wood economic spectrum) that consider traits across species has been slow in  
<sup>19</sup> part because of high trait variation within-species, which is especially high for phenology. Addressing  
<sup>20</sup> this requires data on many traits across space and better estimates of phenology, which is less variable  
<sup>21</sup> when determined through experiments that can be used to decompose its environmental drivers (such  
<sup>22</sup> as chilling and forcing temperatures or photoperiod). Here, working across eight forest communities to  
<sup>23</sup> collect *in situ* trait measurements from 1428 individuals of 47 species, we find phenology connects to  
<sup>24</sup> four major plant functional traits (height, diameter, leaf mass area and nitrogen content) via responses  
<sup>25</sup> to photoperiod, but not temperature. These results provide insight into the complexity of phenology-  
<sup>26</sup> trait relationships in relation to cues, as well as novel support for the inclusion of phenology in studies  
<sup>27</sup> of woody plant growth to accurately forecasts changes in species growth with climate change.

<sup>28</sup> **Introduction**

<sup>29</sup> Climate change is causing species phenologies—the timing of life history events—to shift, with widespread  
<sup>30</sup> advances being observed across the tree of life (Parmesan and Yohe, 2003; Hoegh-Guldberg et al., 2018).  
<sup>31</sup> This common phenological fingerprint, however, averages over high variability across species (Thack-  
<sup>32</sup> eray et al., 2016; Cohen et al., 2018; Kharouba et al., 2018), posing a challenge to accurate forecasts.

<sup>33</sup>

39 In plants, species variation can be explained, in part, by differences in growth strategies, which are generally inferred from traits (Violle et al., 2007). Decades of research on plant traits have worked to build  
40 predictive models of species responses to their environment (Green et al., 2022), which could explain  
41 species-level variability in phenological responses. Phenology, however, has generally been excluded from  
42 plant trait research due to its high inter- and intra-specific variability, making it difficult to leverage  
43 existing frameworks to explain phenological variation and predictions future changes. Previous studies  
44 have found high variation in phenology in observational studies—even for the same species when ob-  
45 served over different years or sites (Primack et al., 2009; Chuine et al., 2010), but variation is usually  
46 much smaller when calculated from controlled experiments, which suggest that phenological variation  
47 can be consistently decomposed into its environmental cues (e.g., temperature and photoperiod Chuine  
48 and Cour, 1999; Harrington and Gould, 2015; Flynn and Wolkovich, 2018).

49 Correlations between plant traits, growth strategies, and responses to environments have been synthe-  
50 sized into several global frameworks, including the leaf economic spectrum (Wright et al., 2004) and  
51 wood economic spectrum (Chave et al., 2009). These frameworks have identified key traits that ex-  
52 hibit distinct gradients, ranging from acquisitive strategies—fast growing plants that produce cheaper  
53 tissue—to conservative strategies—with plants that invest in long-lived tissue but slower growth rates  
54 (Wright et al., 2004; Díaz et al., 2016). In temperate systems, changes in temperature and frost risk in  
55 spring can produce gradients in abiotic stress, including frost risk, soil nutrients, and light availability  
56 (Sakai and Larcher, 1987; Gotelli and Graves, 1996; Augspurger, 2009), in addition to differences in  
57 biotic interactions from herbivory or competition later in the season (Lopez et al., 2008; Wolkovich  
58 and Ettinger, 2014). Species that vary in their timing of leafout, should therefore exhibit traits and  
59 growth strategies that allow them to tolerate or avoid these abiotic and biotic factors. Leveraging in-  
60 sights from predictive models of phenology with these well established trait frameworks could begin to  
61 disentangle the environmental cues that shape phenology from those shaped by other trait differences  
62 in plant growth strategies.

63

64 To determine whether phenology fits within major functional trait frameworks requires working across  
65 within and between species variation. Phenological variation is generally observed in natural con-  
66 ditions where the environmental cues that trigger many phenological events—primarily temperature  
67 and photoperiod (Chuine, 2000; Körner and Basler, 2010)—vary across space and time. Within-species  
68 variation also occurs across other plant traits (e.g., leaf and wood structure traits), including across lat-  
69itudinal (Wiemann and Bruce, 2002) and other environmental gradients (Pollock et al., 2012), though  
70 generally to a smaller scale compared to phenology.

71 To better understand how phenology and other traits correlate across species will require methods that  
72 incorporate spatial variation within species.

73

74 Here, we tested whether phenological variation was aligned with existing trait frameworks using data  
75 on spring budburst paired and a suite of traits that capture acquisitive to conservative growth strate-  
76 gies. We decompose the high phenological variation in budburst date by using experiments to estimate  
77 three major phenological cues for woody plant budburst: chilling (cool winter temperatures), forcing  
78 (warm spring temperatures), and photoperiod.

79

80 We predict that early spring species will budburst before canopy closure exhibited as smaller responses  
81 to temperature and photoperiod. These species should have traits associated with acquisitive growth,  
82 particularly shorter heights, smaller trunk or stem diameters, with lower investment in wood structure  
83 and leaf tissue, resulting in low wood specific density, diffuse-porous wood anatomy, and low leaf mass  
84 area, but high leaf nitrogen content for a greater photosynthetic potential. In contrast, we predict  
85 species with later budburst to predominately include canopy species that express more conservative  
86 growth strategies and require more chilling, warmer forcing, and longer photoperiods. These species  
87 should incur greater investments in long-lived tissue, with ring-porous wood anatomy, taller heights  
88 and greater diameter, denser wood and high leaf mass area, but low leaf nitrogen content. We then used  
89 a joint-modeling approach to estimate the relationships between these plant traits and phenological  
90

91 responses to cues, while partitioning the variance from species- and population-level differences.

## 92 Materials and Methods

### 93 Field sampling

94 We combined *in situ* trait data with budburst data from two growth chamber cutting experiments  
95 conducted across eastern and western temperate deciduous forests in North America. We collected  
96 both suites of data from populations that span a latitudinal gradient of 4-6° for the eastern and  
97 western communities respectively. We took trait measurements from across eight populations, of  
98 which there were four eastern populations—Harvard Forest, Massachusetts, USA (42.55°N, 72.20°W),  
99 White Mountains, New Hampshire, USA (44.11°N, 52.14°W), Second College Grant, New Hampshire,  
100 USA (44.79°N, 50.66°W), and St. Hippolyte, Quebec, Canada (45.98°N, 74.01°W), and four western  
101 population—E.C. Manning Park (49.06°N, 120.78°W), Sun Peaks (50.88°N, 119.89°W), Alex Fraser  
102 Research Forest (52.14°N, 122.14°W), and Smithers (54.78°N, 127.17°W), British Columbia (BC),  
103 Canada (Fig. 1). For the two growth chamber studies on budburst phenology, we collected cuttings  
104 from the most southern and northern populations in each transect ( $n_{pop}=4$ ).  
105

### 106 Functional traits

107 We measured all traits in the summer prior to each growth chamber study (eastern transect: 8-25 June  
108 2015, western transect: 29 May to 30 July 2019), following full leafout but before budset. At each  
109 population and for each species, we measured a total of five traits from 1-10 healthy adult individuals:  
110 height, diameter of the main trunk or stem (hereafter referred to as diameter), wood specific density,  
111 leaf mass area, and the percent leaf nitrogen content. We also obtained xylem structure data from the  
112 WSL xylem database (Schweingruber and Landolt, 2010) for 72.3% of our species.  
113

114 We measured traits in accordance to the methods discussed by Pérez-Harguindeguy et al. (2013).  
115 We calculated tree height using trigonometric methods and used a base height of 1.37 m to measure  
116 diameter (Magarik et al., 2020). For shrub heights, we measured the distance from the ground to the  
117 height of the top foliage and measured stem diameters at approximately 1 cm above ground-level. All  
118 stem and leaf samples were kept cool during transport and measurements of leaf area and stem volume  
119 taken within 3 and 12 hours of sample collection respectively. To measure wood specific density, we  
120 collected a 10 cm sample of branch wood, taken close to the base of the branch at the stem and  
121 calculated stem volume using the water displacement method. For our leaf traits, we haphazardly  
122 selected and sampled five, fully expanded, and hardened leaves, with no to minimal herbivore damage.  
123 We took a high resolution scan of each leaf using a flatbed scanner and estimated leaf area using the  
124 ImageJ software (version 2.0.0).

### 125 Growth chamber study

126 For our growth chamber studies, we collected branch cuttings from our highest and lowest latitude  
127 populations in each transect, with sampling in our eastern study occurring from 20-28 January 2015  
128 and sampling for our western study from 19-28 October 2019. In both studies, we included a total of  
129 eight distinct treatments consisting of two levels of chilling, forcing, and photoperiods (Fig. 1). We  
130 recorded budburst stages of each sample every 1-3 days for up to four months, defining the day of  
131 budburst as the day of budbreak or shoot elongation (denoted as code 07 by Finn et al. (2007)). For  
132 a more detailed discussion of study sample collection and methods see Flynn and Wolkovich (2018)  
133 for details on our eastern study and Loughnan and Wolkovich (in prep) for details on our western study.  
134

135 **Statistical Analysis**

136 Our analysis combined our *in situ* trait data with budburst data from the controlled environment. For  
 137 each trait, we developed a joint Bayesian model, in which the relationship between traits and cues  
 138 is used to estimate budburst. This statistical approach improves upon previous analyses of multiple  
 139 traits, as it allows us to carry through uncertainty between trait and phenology data—and better  
 140 partitions the drivers of variation in species phenologies

141

142 Our joint model consists of two parts. The first is a hierarchical linear model, which partitions the vari-  
 143 ation of individual observations ( $i$ ) of a given trait value ( $Y_{\text{trait}}$ ) to account for the effects of species  
 144 ( $j$ ), population-level differences arising from transects, latitude, as well as the interaction between  
 145 transects and latitude ( $\text{transect} \cdot \text{latitude}$ ), and finally, residual variation or ‘measurement error’ ( $\sigma_m^2$ ).  
 146

$$Y_{\text{trait}_{i,j}} \sim \text{Normal}(\mu_{i,j}, \sigma_m^2) \quad (1)$$

$$\mu_{i,j} = \alpha_{\text{grand trait}} + \alpha_{\text{trait}_j} + \beta_{\text{transect}} \times \text{transect} + \quad (2)$$

$$\beta_{\text{latitude}} \times \text{latitude} + \beta_{\text{transect} \cdot \text{latitude}} \times (\text{transect} \cdot \text{latitude}) \quad (3)$$

(4)

147

$$\boldsymbol{\alpha}_{\text{trait}} \begin{bmatrix} \alpha_{\text{trait}_1} \\ \alpha_{\text{trait}_2} \\ \dots \\ \alpha_{\text{trait}_n} \end{bmatrix} \text{ such that } \boldsymbol{\alpha}_{\text{trait}} \sim \text{Normal}(0, \sigma_{\text{trait}}^2) \quad (5)$$

(6)

148 We include transect as a dummy variable (0/1) and latitude as a continuous variable in our model.  
 149 We modeled traits using their original units, with the exception of leaf mass area and wood specific  
 150 density, which were rescaled by 100 for numeric stability in the model. Our model also includes  
 151 partial pooling for species—which controls for variation in the number of trait estimates per species  
 152 and trait variability—using these species-level estimates as predictors for each cue ( $\beta_{\text{chilling},j}$ ,  $\beta_{\text{forcing},j}$ ,  
 153  $\beta_{\text{photoperiod},j}$ ).

154

$$\beta_{\text{chilling}_j} = \alpha_{\text{chilling},j} + \beta_{\text{trait.chilling}} \times \alpha_{\text{trait},j} \quad (7)$$

$$\beta_{\text{forcing}_j} = \alpha_{\text{forcing},j} + \beta_{\text{trait.forcing}} \times \alpha_{\text{trait},j}$$

$$\beta_{\text{photoperiod}_j} = \alpha_{\text{photoperiod},j} + \beta_{\text{trait.photoperiod}} \times \alpha_{\text{trait},j}$$

155 In addition to the species-level estimates, the second part of our model estimates the overall effect of  
 156 each trait on each cue ( $\beta_{\text{trait.chilling}}$ ,  $\beta_{\text{trait.forcing}}$ ,  $\beta_{\text{trait.photoperiod}}$ ). From this we can estimate how well  
 157 traits explain species-level differences—by estimating the the species-level cue variation not explained  
 158 by traits ( $\alpha_{\text{chilling},j}$ ,  $\alpha_{\text{forcing},j}$ ,  $\alpha_{\text{photoperiod},j}$ ) and individual species responses to cues (*chilling*, *forcing*,  
 159 *photoperiod*, respectively). Finally, our model estimates the residual budburst variation across species  
 160 ( $Y_{\text{pheno},j}$ ), observations ( $\sigma_d^2$ ), as well as the variation in cues not attributed to the trait (using partial  
 161 pooling).

$$Y_{\text{pheno}_{i,j}} \sim \mathcal{N}(\mu_{i,j}, \sigma_d^2) \quad (8)$$

<sup>162</sup> with

$$\mu_{i,j} = \alpha_{\text{pheno}_j} + \beta_{\text{chilling}_j} \cdot \text{chilling} + \beta_{\text{forcing}_j} \cdot \text{forcing} + \beta_{\text{photoperiod}_j} \cdot \text{photoperiod} \quad (9)$$

<sup>163</sup> where  $\alpha_{\text{pheno}_j}$ ,  $\alpha_{\text{chilling}_j}$ ,  $\alpha_{\text{forcing}_j}$ , and  $\alpha_{\text{photoperiod}_j}$  are elements of the normal random vectors:

$$\boldsymbol{\alpha}_{\text{pheno}} = \begin{bmatrix} \alpha_{\text{pheno}_1} \\ \alpha_{\text{pheno}_2} \\ \dots \\ \alpha_{\text{pheno}_n} \end{bmatrix} \text{ such that } \boldsymbol{\alpha}_{\text{pheno}} \sim \text{Normal}(\mu_{\text{pheno}}, \sigma^2_{\text{pheno}}) \quad (10)$$

$$\boldsymbol{\alpha}_{\text{chilling}} = \begin{bmatrix} \alpha_{\text{chilling}_1} \\ \alpha_{\text{chilling}_2} \\ \dots \\ \alpha_{\text{chilling}_n} \end{bmatrix} \text{ such that } \boldsymbol{\alpha}_{\text{chilling}} \sim \text{Normal}(\mu_{\text{chilling}}, \sigma^2_{\text{chilling}}) \quad (11)$$

$$\boldsymbol{\alpha}_{\text{forcing}} = \begin{bmatrix} \alpha_{\text{forcing}_1} \\ \alpha_{\text{forcing}_2} \\ \dots \\ \alpha_{\text{forcing}_n} \end{bmatrix} \text{ such that } \boldsymbol{\alpha}_{\text{forcing}} \sim \text{Normal}(\mu_{\text{forcing}}, \sigma^2_{\text{forcing}}) \quad (12)$$

$$\boldsymbol{\alpha}_{\text{photoperiod}} = \begin{bmatrix} \alpha_{\text{photoperiod}_1} \\ \alpha_{\text{photoperiod}_2} \\ \dots \\ \alpha_{\text{photoperiod}_n} \end{bmatrix} \text{ such that } \boldsymbol{\alpha}_{\text{photoperiod}} \sim \text{Normal}(\mu_{\text{photoperiod}}, \sigma^2_{\text{photoperiod}}) \quad (13)$$

(14)

<sup>164</sup> We modeled each trait individually, with the exception of ring-porosity, which we compared across  
<sup>165</sup> species using the posterior estimates of our wood stem density model, allowing us to account for inher-  
<sup>166</sup> ent differences in wood anatomy across species and growth form. We included all three cues (chilling,  
<sup>167</sup> forcing, and photoperiod) as continuous variables in our model, as well as all two-way interactions  
<sup>168</sup> between cues and between cues and sites. We converted chilling temperatures to total chill portions,  
<sup>169</sup> including both the chilling experienced in the field prior to sampling and during the experiment. For  
<sup>170</sup> this we used local weather station data and the chillR package (v. 0.73.1, Luedeling, 2020). To account  
<sup>171</sup> for differences in thermoperiodicity between the two studies (Buonaiuto et al., 2023), we also converted  
<sup>172</sup> forcing temperatures to mean daily temperatures for each treatment. Finally, we *z*-scored each cue  
<sup>173</sup> and site using two standard deviations to allow direct comparisons between results across parameters  
<sup>174</sup> (Gelman, 2008).

<sup>175</sup>

<sup>176</sup> For each model we used trait specific priors that were weakly informative. We validated our choice  
<sup>177</sup> of priors using prior predictive checks and confirmed model stability under wider priors. All models  
<sup>178</sup> were coded in the Stan programming language for Bayesian models using the rstan package (Stan  
<sup>179</sup> Development Team, 2018) in R version 4.3.1 (R Development Core Team, 2017). All models met basic  
<sup>180</sup> diagnostic checks, including no divergences, high effective sample sizes ( $n_{eff}$ ) that exceeded 10% of  
<sup>181</sup> the number of iterations, and  $\hat{R}$  values close to 1. We report our model estimates as the mean values  
<sup>182</sup> with 90% uncertainty intervals (UI), interpreting parameter estimates with intervals that overlap to  
<sup>183</sup> be statistically similar to each other and those that include zero to have small effects.

<sup>184</sup>

## <sup>185</sup> Results

<sup>186</sup> Across our eight populations, we measured 47 species of which 28 were in our eastern transect and  
<sup>187</sup> 22 in our western transect. These include species dominant in both the understory and canopy layer,

188 with our eastern community consisting of 13 shrubs and 15 trees, our western community consisting of  
189 18 shrubs and 4 trees, and three species that occurred in both transects. In total we measured traits  
190 of 1428 unique individuals between the two transects across our five *in situ* traits: height ( $n = 1317$ ),  
191 diameter ( $n = 1220$ ), wood stem density ( $n = 1359$ ), leaf mass area ( $n = 1345$ ), leaf nitrogen con-  
192 tent ( $n = 1351$ ). Across our two growth chamber studies, we made observations of 4211 samples, with  
193 our observations of budburst spanning 82 and 113 days for our eastern and western studies respectfully.  
194

195 Most of our traits showed some variation by latitude within each transect, with a strong interactive  
196 effect between transect and latitude (Fig. 2). Leaf nitrogen content was the only trait to vary with  
197 latitude alone, with low latitude communities on both our eastern and western transects having greater  
198 values of leaf nitrogen content than communities at higher latitudes (-0.1, UI: -0.2, 0.0, Table S6).  
199 The strongest negative interaction was observed for height (-0.2, UI: -0.4, 0.0), while the strongest  
200 positive interaction was observed for leaf mass area (0.5, UI: 0.4, 0.6). Height and wood stem density  
201 both exhibited negative transect by latitude interactions (-0.2, UI: -0.4, 0.0 for our height model and  
202 -0.1, UI: -0.2, -0.1 for our wood stem density model), with woody species in our eastern communities  
203 exhibited greater heights and wood stem densities with increasing latitude, but decreasing values with  
204 latitude in our western communities (Fig. 2 a and c). In contrast, diameter and leaf mass area both  
205 exhibited positive transect by latitude interactions (0.5, UI: 0.1, 0.9 for our diameter model and 0.5,  
206 UI: 0.4, 0.6 for our leaf mass area model), with plants at higher latitudes having increasing diameters in  
207 both our eastern and western communities but decreasing leaf mass areas in our eastern communities  
208 and increasing values in our western communities (Fig. 2 b and d). In addition to the differences we  
209 found across populations, we also observed considerable differences between individual species, which  
210 varied considerably and up to 7 fold for some traits (Fig. 3).

211 We found that three of our four traits had a strong relationship with photoperiod, but not always in  
212 the direction we predicted. Taller species with larger trunk diameters and leaves with high nitrogen  
213 content had larger responses with longer photoperiods (Fig. 3 c, i, o; Tables S2, S3, S6). But, contrary  
214 to our expectation, species with denser, high leaf mass area leaves had smaller photoperiod responses,  
215 allowing them to potentially budburst under shorter photoperiods (Fig. 3f).

216 Temperature cues ( $\beta_{\text{trait.chilling}}$  and  $\beta_{\text{trait.forcing}}$ ) exhibited no relationships with individual traits, but  
217 by accounting for the effects of leaf or wood traits, we found the importance of our three cues to vary  
218 by trait. Chilling ( $\beta_{\text{chilling}}$ ) was the strongest cue of budburst in our models of height (-13.4 m per  
219 standardized chill portions, UI: -17.2, -9.9), diameter (-12.5 cm per standardized chill portions, UI:  
220 -16.2, -8.6), wood stem density (-20.9 g/cm<sup>2</sup> per standardized chill portions, UI: -33.2, -9.8), and leaf  
221 nitrogen content (-35.1 percent per standardized chill portions, UI: -68.1, -4.1), with more chilling  
222 advancing budburst. Our model of leaf mass area, however, estimated photoperiod as the strongest  
223 cue ( $\beta_{\text{photoperiod}}$ , -14.0, UI: -23.1, -3.5). After accounting for the effects of traits, only our height and  
224 diameter model found all three environmental cues to drive budburst timing (Tables S2, S3). Our  
225 models of wood stem density and leaf nitrogen content in turn found temperature cues alone to shape  
226 budburst (Tables S4, S6), while our model of leaf mass area found a large response to only photoperiod  
227 (Table S5).

228 In synthesizing the effects of multiple traits across species, our results can be used to make general-  
229 izations across ecologically important groups of species. But only some of our models estimated clear  
230 gradients in species timing between trees and shrubs. In particular, we found height to have large  
231 correlations between budburst timing and trait values, with earlier estimates of budburst for shrubs  
232 (with a mean day of budburst of 10)—especially under greater cues—and later budburst estimates  
233 for trees (with a mean day of budburst of 17.3, Fig. S1). Diameter at breast height showed similar  
234 trends as estimates from our height model (results not shown). But this was not the case for our two  
235 leaf traits. Leaf nitrogen content, for example, showed no distinct separation between shrub and tree  
236 functional groups (Fig. S1).

## 241 Discussion

242 Using our joint modeling approach, we estimated how leaf and wood traits interact with temperature  
 243 and photoperiod cues to shape species budburst. We found that photoperiod—often the weakest cue  
 244 of budburst (Laube et al., 2014; Zohner et al., 2016; Flynn and Wolkovich, 2018)—was the most im-  
 245 portant cue in trait-phenology relationships. In general, we also found trait patterns varied between  
 246 our eastern and western transects and with latitude. These spatial differences in trait variation may be  
 247 due to differences in the community assemblages, as our western community is more shrub dominated,  
 248 with shorter plants with less dense branch wood. This more acquisitive growth strategy suggests these  
 249 species are more likely to utilize resources early in the season prior to canopy closure. **Collectively our**  
 250 **results provide new insights into the complex tradeoffs between cues and traits and how they differ**  
 251 **across large spatial scales.**

252

## 253 Cues and functional traits

254 We found only partial support for our prediction that species with acquisitive traits—particularly  
 255 small trees with low wood density, low leaf mass area, and high leaf nitrogen content—would have  
 256 early budburst via smaller temperature and photoperiod responses. We did find species with smaller  
 257 heights and diameters to have smaller photoperiod responses. But contrary to our prediction, species  
 258 with less dense leaves showed larger responses to photoperiod, while leaves with high nitrogen content  
 259 had stronger photoperiod responses. None of our focal traits, however, showed a relationship with tem-  
 260 perature (chilling or forcing), which may be due to selection on other physiological processes. Many of  
 261 our traits are associated with one or more ecological function (Wright et al., 2004; Pérez-Harguindeguy  
 262 et al., 2013; Reich, 2014). In particular, leaf mass area is known to correlate with traits like leaf lifespan  
 263 or decomposition rates in addition to light capture (De La Riva et al., 2016). While our results high-  
 264 light the ways in which phenology partially aligns with gradients found in established trait frameworks,  
 265 they also offer new insight into potential tradeoffs in how varying physiological processes shape species  
 266 growth strategies.

267

268 Decades of previous phenology research have found budburst timing to be primarily driven by tem-  
 269 perature (chilling and forcing) and weakly by photoperiod (Chuine et al., 2010; Basler and Körner,  
 270 2014; Laube et al., 2014). But we found no other traits that correlate with responses to temperature,  
 271 **suggesting other cues or biotic interactions** may impact leaf and structural traits in temperate forests.  
 272 Leaf mass area also varies with soil moisture, with variation in leaf area allowing plants to reduce  
 273 evaporation under dry conditions, and thus selecting for high trait values (De La Riva et al., 2016).  
 274 Soil moisture also shapes other phenological events in woody plants, including radial growth phenology  
 275 and shoot elongation (Cabon et al., 2020; Peters et al., 2021). If selection by soil moisture is shaping  
 276 phenological responses, it may be contributing to the unexpected trends we observed in leaf traits  
 277 and the absence of relationships with temperature. **To fully understand how species growth strategies**  
 278 **correlate with phenology may thus require additional environmental cues to be considered.**

279

280 The absence of trait-cue relationships between budburst and wood structure and wood stem density  
 281 contrasts the findings of previous work linking these traits. Previous studies have found some evidence  
 282 that trees with diffuse-porous wood structure leafout earlier than species with ring-porous structures  
 283 (Lechowicz, 1984; Panchen et al., 2014; Yin et al., 2016; Osada, 2017; Savage et al., 2022). Using  
 284 wood density as alternative measure of wood structure (wood density positively correlates with xylem  
 285 resistance to embolism, Hacke et al., 2001), we did not find clear association between our three pheno-  
 286 logical cues and xylem structure, despite our data also focusing on species in temperate forests. **Most**

287 of the individuals we measured, however, did have a fairly narrow range of wood specific densities  
288 (varying from 0.2 to 0.6 g/cm<sup>3</sup>) relative to the variation in wood density observed in studies that  
289 focus on tropical species or span a more global distribution (?Savage et al., 2022; ?). We did find  
290 some variation in wood density across our different sites and with latitude. The larger wood densities  
291 we observed at higher latitudes in our eastern transect could be caused by the differences in winter  
292 conditions experienced by canopy versus understory species. The canopy tree species that dominate  
293 our eastern communities may experience greater horizontal stress from wind and downward pressure  
294 from snow, explaining the greater wood densities they exhibit at higher latitudes (MacFarlane and  
295 Kane, 2017; MacFarlane, 2020), while species in the shrub dominated western communities experience  
296 greater protection from being in the understory.

297

298 In comparing our results with a global meta-analysis of tree trait relationships with budburst cues  
299 (Loughnan et al., 2025), we found similar trait-cue relationships for height and leaf mass area. At  
300 both the global and continental scales, we found taller tree heights to leafout with longer photoperiods.  
301 We also found species with high specific leaf area—which is the inverse of leaf mass area and  
302 thus equivalent to low values—exhibited large responses to photoperiod (Loughnan et al., 2025). The  
303 consistency of these results, despite the differences in the two spatial scales of these datasets, provides  
304 further evidence that alternate underlying mechanisms are shaping how woody species respond to  
305 photoperiod cues.

306

### 307 **Functional traits predict climate change responses**

308 Our results offer novel insights into how broader correlations between growth strategies and phenological  
309 cues can help predict responses in woody plant communities with climate change. As temperatures  
310 rise, particularly at higher latitudes (Hoegh-Guldberg et al., 2018), warmer winter and spring temper-  
311 atures may select for earlier budburst in some species. But, since photoperiod will remain fixed, our  
312 observed relationships between photoperiod and other traits has the potential to limit species abilities  
313 to track temperatures. This could constrain the extent to which some species growth will advance with  
314 climate change. Our results suggest that these effects will likely be greater for taller species or canopy  
315 trees and species with relatively low leaf mass area. These constraints could have cascading effects  
316 on forest communities, as variable species responses to increasing temperatures further alter species  
317 growth strategies and their interactions with competitors or herbivores within their communities.

318

319 Our findings of correlations between phenology and other commonly measured traits highlight how  
320 accurate forecasts of future changes in phenology can benefit from accounting for the response of other  
321 traits to climate change. Across temperature and precipitation gradients, leaf size and shape also  
322 change, as species shift to conserve water and mitigate effects of transpiration under higher temper-  
323 atures (De La Riva et al., 2016). These changes could impact species photosynthetic potential and  
324 ultimately ecosystem services, such as carbon sequestration. While phenological research has focused  
325 on forecasting responses to temperature, the correlation of other traits with photoperiod suggests it is  
326 also an important cue. By considering the tradeoffs and differences in cues that simultaneously shape  
327 plants growth strategies, we can more accurately forecast species phenology and community dynamics  
328 under future climates.

329

## 330 **References**

- 331 Augspurger, C. K. 2009. Spring 2007 warmth and frost: phenology, damage and refoliation in a  
332 temperate deciduous forest. *Functional Ecology* 23:1031–1039.

- 333 Basler, D., and C. Körner. 2014. Photoperiod and temperature responses of bud swelling and bud  
334 burst in four temperate forest tree species. *Tree Physiology* 34:377–388.
- 335 Buonaiuto, D. M., E. M. Wolkovich, and M. J. Donahue. 2023. Experimental designs for testing the  
336 interactive effects of temperature and light in ecology : The problem of periodicity. *Functional  
337 Ecology* 37:1747–1756.
- 338 Cabon, A., L. Fernández-de-Uña, G. Gea-Izquierdo, F. C. Meinzer, D. R. Woodruff, J. Martínez-  
339 Vilalta, and M. De Cáceres. 2020. Water potential control of turgor-driven tracheid enlargement in  
340 Scots pine at its xeric distribution edge. *New Phytologist* 225:209–221.
- 341 Chave, J., D. Coomes, S. Jansen, S. L. Lewis, N. G. Swenson, and A. E. Zanne. 2009. Towards a  
342 worldwide wood economics spectrum. *Ecology Letters* 12:351–366.
- 343 Chuine, I. 2000. A unified model for budburst of trees. *Journal of Theoretical Biology* 207:337–347.
- 344 Chuine, I., and P. Cour. 1999. Climatic determinants of budburst seasonality in four temperate-zone  
345 tree species. *New Phytologist* 143:339–349.
- 346 Chuine, I., X. Morin, and H. Bugmann. 2010. Warming, photoperiods, and tree phenology. *Science*  
347 329:277–278.
- 348 Cohen, J. M., M. J. Lajeunesse, and J. R. Rohr. 2018. A global synthesis of animal phenological  
349 responses to climate change. *Nature Climate Change* 8:224–228.
- 350 De La Riva, E. G., M. Olmo, H. Poorter, J. L. Uberta, and R. Villar. 2016. Leaf Mass per Area (LMA)  
351 and Its Relationship with Leaf Structure and Anatomy in 34 Mediterranean Woody Species along a  
352 Water Availability Gradient. *PLOS ONE* 11:e0148788.
- 353 Diaz, S., J. Kattge, J. H. C. Cornelissen, I. J. Wright, S. Lavorel, S. Dray, B. Reu, M. Kleyer, C. Wirth,  
354 I. Colin Prentice, E. Garnier, G. Bönisch, M. Westoby, H. Poorter, P. B. Reich, A. T. Moles, J. Dickie,  
355 A. N. Gillison, A. E. Zanne, J. Chave, S. Joseph Wright, S. N. Sheremet'ev, H. Jactel, C. Baraloto,  
356 B. Cerabolini, S. Pierce, B. Shipley, D. Kirkup, F. Casanoves, J. S. Joswig, A. Günther, V. Falcuk,  
357 N. Rüger, M. D. Mahecha, and L. D. Gorné. 2016. The global spectrum of plant form and function.  
358 *Nature* 529:167–171.
- 359 Finn, G. A., A. E. Straszewski, and V. Peterson. 2007. A general growth stage key for describing trees  
360 and woody plants. *Annals of Applied Biology* 151:127–131.
- 361 Flynn, D. F. B., and E. M. Wolkovich. 2018. Temperature and photoperiod drive spring phenology  
362 across all species in a temperate forest community. *New Phytologist* 219:1353–1362.
- 363 Gelman, A. 2008. Scaling regression inputs by dividing by two standard deviations. *Statistics in  
364 Medicine* 27:2865–2873.
- 365 Gotelli, N. J., and G. R. Graves. 1996. The temporal niche. Pages 95–112 in Null Models In Ecology.  
366 Smithsonian Institution Press, Washington, D. C.
- 367 Green, S. J., C. B. Brookson, N. A. Hardy, and L. B. Crowder. 2022. Trait-based approaches to  
368 global change ecology: moving from description to prediction. *Proceedings of the Royal Society B:  
369 Biological Sciences* 289:1–10.
- 370 Hacke, U. G., J. S. Sperry, W. T. Pockman, S. D. Davis, and K. A. McCulloh. 2001. Trends in wood  
371 density and structure are linked to prevention of xylem implosion by negative pressure. *Oecologia*  
372 126:457–461.
- 373 Harrington, C. A., and P. J. Gould. 2015. Tradeoffs between chilling and forcing in satisfying dormancy  
374 requirements for Pacific Northwest tree species. *Frontiers in Plant Science* 6:1–12.

- 375 Hoegh-Guldberg, O., D. Jacob, M. Taylor, M. Bind, S. Brown, I. Camilloni, A. Diedhiou, R. Djalante,  
376 K. Ebi, F. Engelbrecht, J. Guiot, Y. Hijioka, S. Mehrotra, A. Payne, S. Seneviratne, A. Thomas,  
377 R. Warren, and G. Zhou. 2018. Impacts of 1.5 °C Global Warming on Natural and Human Systems.  
378 In: Global Warming of 1.5 °C. An IPCC Special Report on the impacts of global warming of 1.5 °C  
379 above pre-industrial levels and related global greenhouse gas emission pathways, in the context of .  
380 Tech. rep., Cambridge University Press, Cambridge, UK and New York, NY, USA.
- 381 Kharouba, H. M., J. Ehrlén, A. Gelman, K. Bolmgren, J. M. Allen, S. E. Travers, and E. M. Wolkovich.  
382 2018. Global shifts in the phenological synchrony of species interactions over recent decades. Pro-  
383 ceedings of the National Academy of Sciences 115:5211–5216.
- 384 Körner, C., and D. Basler. 2010. Phenology Under Global Warming. *Science* 327:1461–1463.
- 385 Laube, J., T. H. Sparks, N. Estrella, J. Höfler, D. P. Ankerst, and A. Menzel. 2014. Chilling outweighs  
386 photoperiod in preventing precocious spring development. *Global Change Biology* 20:170–182.
- 387 Lechowicz, M. J. 1984. Why Do Temperate Deciduous Trees Leaf Out at Different Times? *Adaptation*  
388 and Ecology of Forest Communities. *The American Naturalist* 124:821–842.
- 389 Lopez, O. R., K. Farris-Lopez, R. A. Montgomery, and T. J. Givnish. 2008. Leaf phenology in relation  
390 to canopy closure in southern Appalachian trees. *American Journal of Botany* 95:1395–1407.
- 391 Loughnan, D., F. A. Jones, G. Legault, C. J. Chamberlain, D. M. Buonaiuto, A. K. Ettinger, M. Gar-  
392 ner, D. S. Sodhi, and E. M. Wolkovich. 2025. Budburst timing within a functional trait framework.  
393 *Journal of Ecology* 00:1–12.
- 394 Loughnan, D., and E. M. Wolkovich. in prep. Temporal assembly of woody plant communities shaped  
395 equally by evolutionary history as by current environments .
- 396 Luedeling, E. 2020. chillR: Statistical Methods for Phenology Analysis in Temperate Fruit Trees.  
397 <https://CRAN.R-project.org/package=chillR>.
- 398 MacFarlane, D. W. 2020. Functional Relationships Between Branch and Stem Wood Density for  
399 Temperate Tree Species in North America. *Frontiers in Forests and Global Change* 3.
- 400 MacFarlane, D. W., and B. Kane. 2017. Neighbour effects on tree architecture: functional trade-offs  
401 balancing crown competitiveness with wind resistance. *Functional Ecology* 31:1624–1636.
- 402 Magarik, Y. A., L. A. Roman, and J. G. Henning. 2020. How should we measure the dbh of multi-  
403 stemmed urban trees? *Urban Forestry & Urban Greening* 47:1–11.
- 404 Osada, N. 2017. Relationships between the timing of budburst, plant traits, and distribution of 24  
405 coexisting woody species in a warm-temperate forest in Japan. *American Journal of Botany* 104:550–  
406 558.
- 407 Panchen, Z. A., R. B. Primack, B. Nordt, E. R. Ellwood, A. Stevens, S. S. Renner, C. G. Willis,  
408 R. Fahey, A. Whittemore, Y. Du, and C. C. Davis. 2014. Leaf out times of temperate woody  
409 plants are related to phylogeny, deciduousness, growth habit and wood anatomy. *New Phytologist*  
410 203:1208–1219.
- 411 Parmesan, C., and G. Yohe. 2003. A globally coherent fingerprint of climate change impacts across  
412 natural systems. *Nature* 421:37–42.
- 413 Pérez-Harguindeguy, N., S. Díaz, E. Garnier, S. Lavorel, H. Poorter, P. Jaureguiberry, M. S. Bret-  
414 Harte, W. K. Cornwell, J. M. Craine, D. E. Gurvich, C. Urcelay, E. J. Veneklaas, P. B. Reich,  
415 L. Poorter, I. J. Wright, P. Ray, L. Enrico, J. G. Pausas, A. C. de Vos, N. Buchmann, G. Funes,  
416 F. Quétier, J. G. Hodgson, K. Thompson, H. D. Morgan, H. ter Steege, M. G. A. van der Heijden,

- 417 L. Sack, B. Blonder, P. Poschlod, M. V. Vaineretti, G. Conti, A. C. Staver, S. Aquino, and J. H. C.  
418 Cornelissen. 2013. New handbook for standardized measurement of plant functional traits worldwide.  
419 Australian Journal of Botany 61:167–234.
- 420 Peters, R. L., K. Steppe, H. E. Cuny, D. J. De Pauw, D. C. Frank, M. Schaub, C. B. Rathgeber,  
421 A. Cabon, and P. Fonti. 2021. Turgor – a limiting factor for radial growth in mature conifers along  
422 an elevational gradient. New Phytologist 229:213–229.
- 423 Pollock, L. J., W. K. Morris, and P. A. Vesk. 2012. The role of functional traits in species distributions  
424 revealed through a hierarchical model. Ecography 35:716–725.
- 425 Primack, R. B., I. Ibáñez, H. Higuchi, S. D. Lee, A. J. Miller-Rushing, A. M. Wilson, and J. A. Silan-  
426 der. 2009. Spatial and interspecific variability in phenological responses to warming temperatures.  
427 Biological Conservation 142:2569–2577.
- 428 R Development Core Team. 2017. R: A language and environment for statistical computing.
- 429 Reich, P. B. 2014. The world-wide ‘fast–slow’ plant economics spectrum: a traits manifesto. Journal  
430 of Ecology 102:275–301.
- 431 Sakai, A., and W. Larcher. 1987. Frost Survival of Plants: Responses and adaptation to freezing stress.  
432 Springer-Verlag, Berlin, Heidelberg.
- 433 Savage, J. A., T. Kiecker, N. McMann, D. Park, M. Rothendler, and K. Mosher. 2022. Leaf out time  
434 correlates with wood anatomy across large geographic scales and within local communities. New  
435 Phytologist 235:953–964.
- 436 Schweingruber, F., and W. Landolt. 2010. The xylem database.
- 437 Stan Development Team. 2018. RStan: the R interface to Stan. R package version 2.17.3.
- 438 Thackeray, S. J., P. A. Henrys, D. Hemming, J. R. Bell, M. S. Botham, S. Burthe, P. Helaouet,  
439 D. G. Johns, I. D. Jones, D. I. Leech, E. B. MacKay, D. Massimino, S. Atkinson, P. J. Bacon,  
440 T. M. Brereton, L. Carvalho, T. H. Clutton-Brock, C. Duck, M. Edwards, J. M. Elliott, S. J. Hall,  
441 R. Harrington, J. W. Pearce-Higgins, T. T. Høye, L. E. Kruuk, J. M. Pemberton, T. H. Sparks,  
442 P. M. Thompson, I. White, I. J. Winfield, and S. Wanless. 2016. Phenological sensitivity to climate  
443 across taxa and trophic levels. Nature 535:241–245.
- 444 Violette, C., M. Navas, D. Vile, E. Kazakou, C. Fortunel, I. Hummel, and E. Garnier. 2007. Let the  
445 concept of trait be functional! Oikos 116:882–892.
- 446 Wiemann, M. C., and W. G. Bruce. 2002. Geographic variation in wood specific gravity: effects of  
447 latitude, temperature, and precipitation. Wood and Fiber Science 34:96–107.
- 448 Wolkovich, E. M., and A. K. Ettinger. 2014. Back to the future for plant phenology research. New  
449 Phytologist 203:1021–1024.
- 450 Wright, I. J., M. Westoby, P. B. Reich, J. Oleksyn, D. D. Ackerly, Z. Baruch, F. Bongers, J. Cavender-  
451 Bares, T. Chapin, J. H. C. Cornelissen, M. Diemer, J. Flexas, J. Gulias, E. Garnier, M. L. Navas,  
452 C. Roumet, P. K. Groom, B. B. Lamont, K. Hikosaka, T. Lee, W. Lee, C. Lusk, J. J. Midgley,  
453 Ü. Niinemets, H. Osada, H. Poorter, P. Pool, E. J. Veneklaas, L. Prior, V. I. Pyankov, S. C.  
454 Thomas, M. G. Tjoelker, and R. Villar. 2004. The worldwide leaf economics spectrum. Nature  
455 428:821–827.
- 456 Yin, J., J. D. Fridley, M. S. Smith, and T. L. Bauerle. 2016. Xylem vessel traits predict the leaf  
457 phenology of native and non-native understorey species of temperate deciduous forests. Functional  
458 Ecology 30:206–214.

- 459 Zohner, C. M., B. M. Benito, J.-C. Svenning, and S. S. Renner. 2016. Day length unlikely to constrain  
460 climate-driven shifts in leaf-out times of northern woody plants. *Nature Climate Change* 6:1120–  
461 1123.

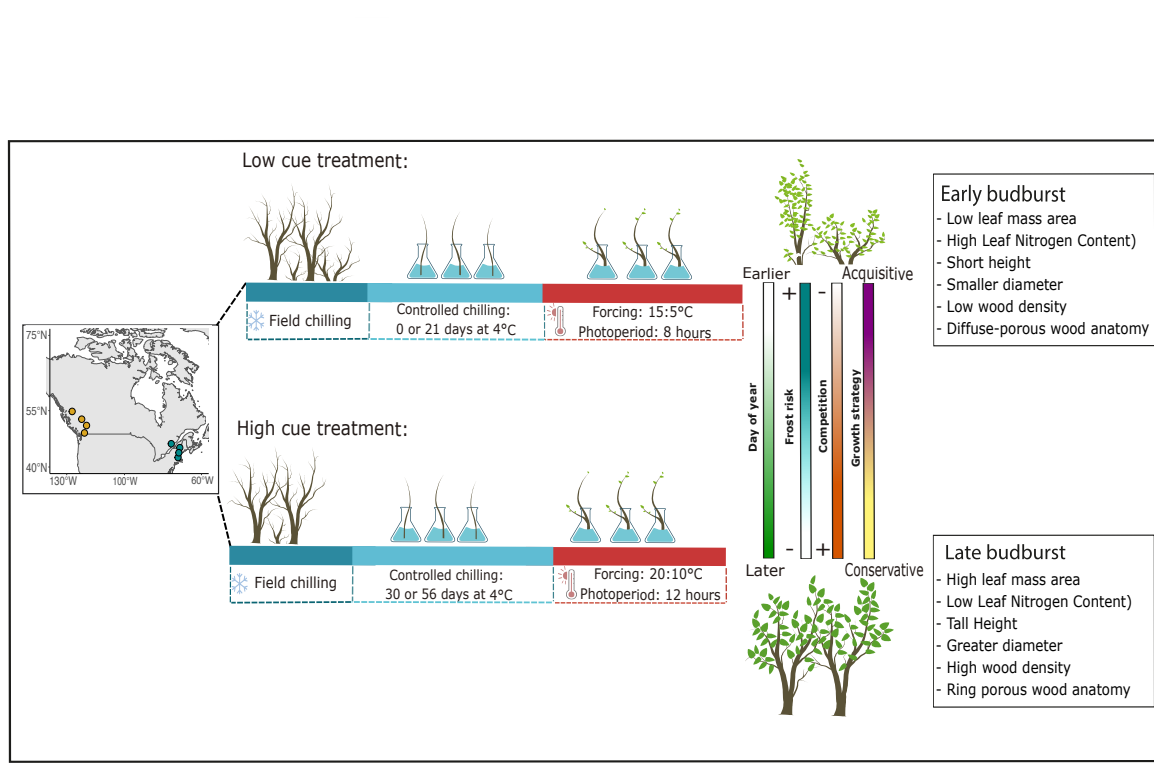


Figure 1: We collected traits data and branch cuttings from plants growing within eight sites, across two transects in eastern and western North America. Cuttings were used in two controlled environment studies in which we applied an high and low chilling, forcing, and photoperiod treatments respectively and recorded the day of budburst of each individual. Using our paired *in situ* trait and experimental budburst data, we tested whether earlier budbursting species exhibited traits associated with more acquisitive growth strategies and smaller responses to cues and later budbursting species a more conservative growth strategy and larger responses to cues.

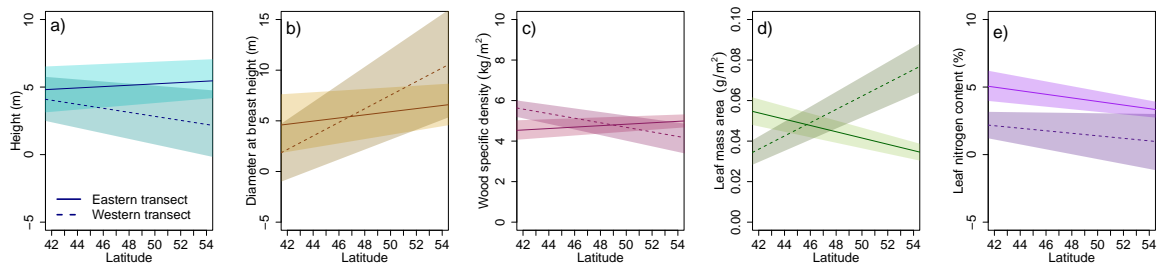


Figure 2: We found a. height, b. diameter, c. branch stem density, and d. leaf mass area to all experience a strong interaction between latitude and transect, e. while leaf nitrogen content showed a strong effect of latitude alone.

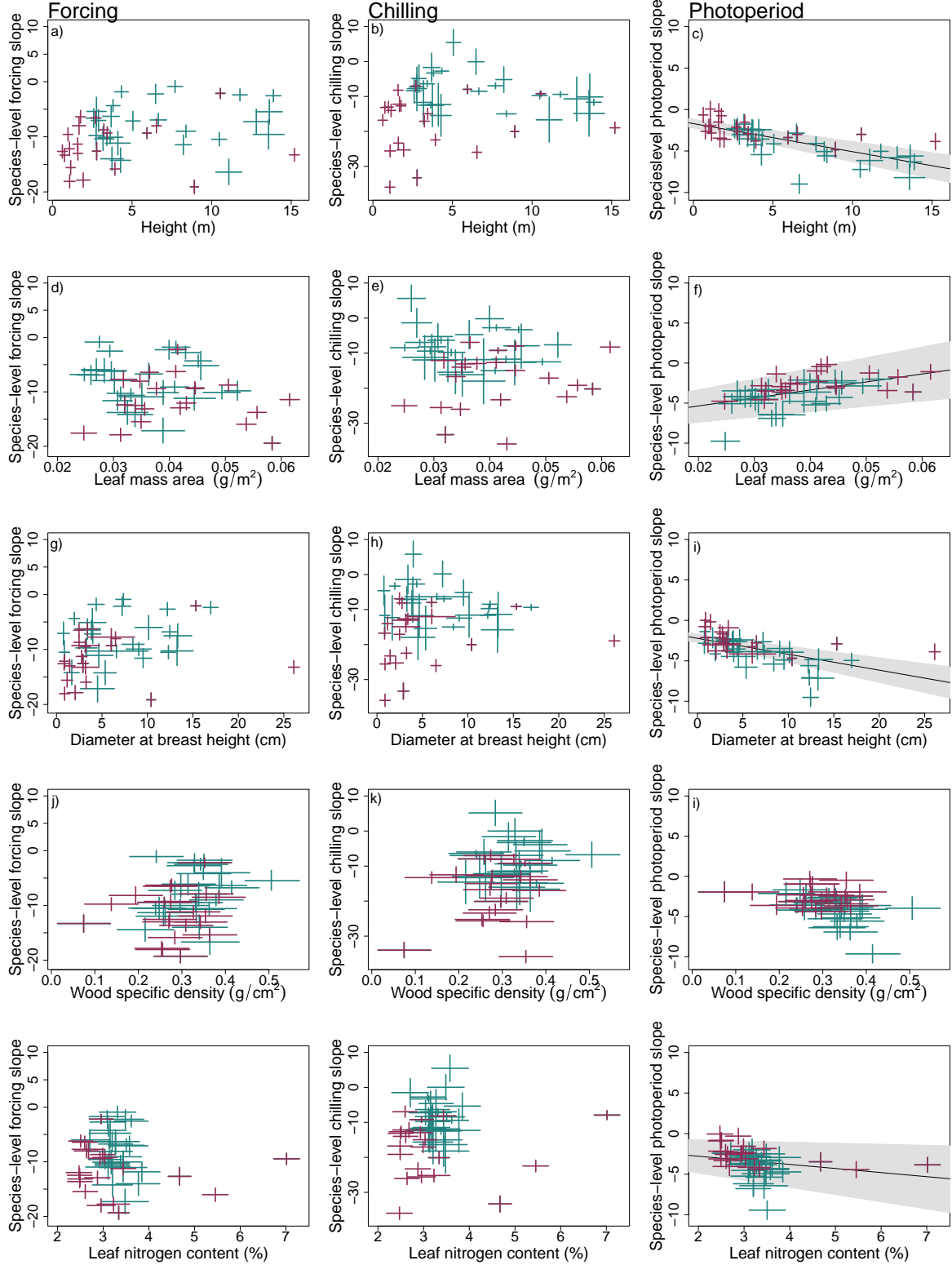


Figure 3: Relationships between species traits and cue responses showed considerable variation across a-c. height, d-f. leaf mass area, g-i. diameter, j-l. wood specific density, and m-o. the leaf nitrogen content. Point colours representing different species groups, with tree species shown in red and shrub species in blue. Crosses depict the 50% uncertainty interval of the model estimates of species trait values and estimated responses to cues. Grey bands depict large relationships between a trait and cue, representing the 90% uncertainty interval, and black lines the mean response.

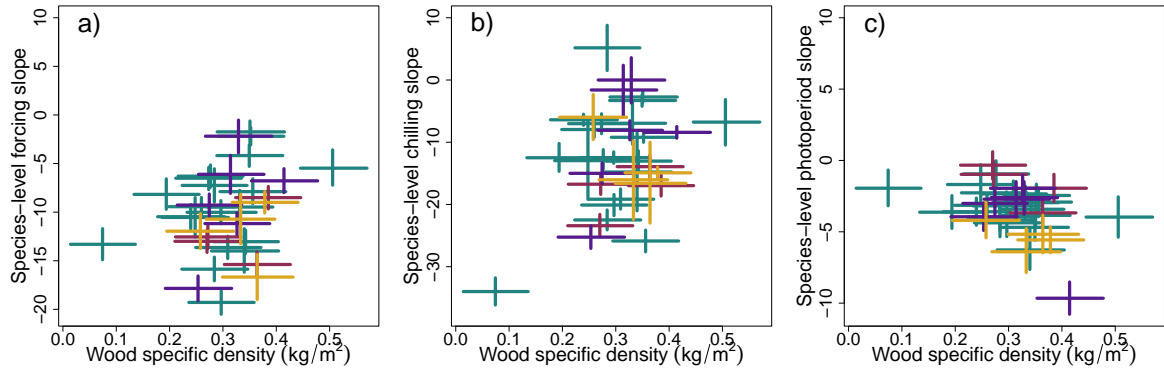


Figure 4: Despite previous studies finding relationships between leaf out timing and species wood xylem structures, we did not find clear differences in species-level estimates of cue responses with wood structure or relative to their wood specific densities. Each cross represents the 50% uncertainty interval of **a.** forcing, **b.** chilling, and **c.** photoperiod responses and wood specific density, with colors depicting different types of wood structure. The lowest wood specific density was observed in *Sambucus racemosa* and the highest wood specific density for *Viburnum lantanoides*.